NUMERICAL INVESTIGATION OF BVI MODELING EFFECTS ON HELICOPTER ROTOR FREE WAKE SIMULATIONS

X. K. Zioutis, A. I. Spyropoulos, D. P. Margaris, D. G. Papanikas
Fluid Mechanics Lab., Mechanical Engineering. and Aeronautics Department,
University of Patras, Greece

Keywords: *helicopter aerodynamics, BVI, rotor wake*

Abstract

This paper presents the influences of numerical Blade Vortex Interactions (BVI) simulation on the computational results of rotor blade downwash distribution and airloading. This investigation is performed on the basis of a developed computational procedure utilizing Vortex Element Method for rotor free wake computations. By these means wake vortices are modeled by a series of discrete vortex elements and induced velocity on rotor disk is calculated for the distorted wake geometry, integrating Biot-Savart law in closed form over each one of them. Bound circulation variations and unsteady blade airloading as a result of the nonuniform induced downwash are computed utilizing a blade element like method. Wake roll up process, vortex core modeling, vorticity dissipation and elastic blade motion are some of the aerodynamic topics modeled with special care in the developed procedure.
Using the computational flexibility of Vortex Element Method, BVI locations are captured and the phenomena are categorized as parallel, perpendicular and oblique regarding their orientation relative to rotor blade. The corresponding intensity and locus for each category are calculated via a lifting surface methodology taking into account compressible blade flowfield. In addition, with the developed procedure the influence of each BVI phenomenon is isolated and its influence on blade downwash and airloads distribution is demonstrated. The computational results of BVIs location and strength distribution on rotor disk, are compared with experimental data of blade airloading for a number of decent and level flight conditions. These data are derived from model-rotor wind tunnel tests, performed in the duration of joined European research programs.

1 Introduction

Among the most important phenomena characterizing helicopter rotor wake are the close encounters of rotor blades with tip vortices, which are known as blade-vortex interactions or BVIs. During these interactions a rotor blade passes close to, or even “hits”, a concentrated vortex and both the local blade surface pressure and the distribution of vorticity in vortex core region are altered. The resulting surface pressure fluctuations produce highly unsteady airloads and intense noise radiation. Thus BVI phenomena have a major impact on blade vibration and are responsible for the characteristic sound of the rotorcraft in flight regimes where blade and wake are in proximity. Because of their significant importance on rotor aerodynamics and acoustics, investigation of BVIs was the subject of several experimental research efforts [1,2,3], aiming to provide better physical understanding of the phenomena. In addition several efforts have been made for the development of computational models to adequately incorporate BVIs in numerical rotor flowfield simulations [4,5,6].

The work reported here aims to present the influence of BVI numerical modeling on predicted rotor airloads, non-uniform downwash and on computed rotor wake geometry. Rotor

blade and wake computations are based on a developed procedure [7] utilizing the free wake concept, with the adoption of Vortex Element Method (VEM) for wake simulation. The overall rotor wake vorticity is assumed to consist of three interacting parts, the concentrated tip vortex and the spread trailing and shed vorticity at the inboard region of the blade. Each of these parts is represented by a multitude of finite vortex elements either of line or surface type. Vortex elements mutual influences and rotor downwash distribution are calculated by integrating individual element contributions on total induced velocity at the corresponding points. Blade dynamics have been adequately incorporated taking into account first mode of flapwise blade bending. Rotor airloads are calculated with the application of a blade element type methodology, which combines lifting line and lifting surface concepts.

In general free wake methods coupled with non-CFD codes for blade calculations is a computationally efficient and relatively accurate procedure compared to consuming 3-D Euler/ Navier Stokes solvers, but special phenomena such as BVI must be modeled with care to improve the effectiveness of the method. Taking advantage of the computational flexibility of the developed procedure, extensive modifications have been made to include detailed BVI simulation. A distinction is made regarding the relative position of blade and interacting vortex, and each BVI event is designated as oblique, parallel or perpendicular [8]. Parallel BVI is usually observed on the advancing side while perpendicular BVI is common over the front and rear of the disk [9]. Appropriate modeling is applied based on theoretical [10] approaches and the results are compared with experimental measurements. The extra shedding of near wake due to local changes in bound circulation is simulated and formulas are developed to calculate the influences on rotor blade. Special attention has been given on modeling BVI effects on vortex core structure and decay, which are important for subsequent interactions of the same vortex and determine the final computed wake geometry. Possible vortex core bursting is examined for every BVI event under specified criteria and its propagation on vortex filament is computationally simulated.

The results of BVI modeling and computational treatment are compared with experimental data for several flight conditions. These data are derived from model-rotor wind tunnel tests performed in the duration of joined European research programs [11].

2 Rotor Aerodynamic Flowfield Analysis

2.1 Free Wake Concept

One of the most important characteristics of helicopter rotor blades is that they tend to stay in close proximity to their wake, long enough to experience significant influences on their aerodynamic performance. This is mainly due to the non-uniform downwash induced on the rotor disk and to the close encounters between the blades and concentrated vortices of rotor wake. These impacts on blade aerodynamics have their corresponding effects on rotor aeroacoustics and as a conclusion any methodology targeting to calculate rotor aerodynamics or acoustics must be based on a reliable simulation of the complicated wake flowfield.

For this purpose, several approaches have been introduced, some of them using CFD methods [12] and others adopting Lagrangian-type techniques such as vortex methods due to Chorin [13] or the "free" wake concept. The later is a continuous improving methodology, which due to recent years research has became a powerful aerodynamic tool for the prediction of rotor induced flowfield [14,15].

The work presented here is based on the free wake concept with the application of Vortex Element Method. Wake vorticity can form either concentrated filaments or distributed surfaces, which are moving randomly in 3D space. The objective of VEM is to simulate these formations of vorticity with simple computational elements, in order to predict the velocity field induced on the rotor disk and in the wake itself. For this purpose discrete straight or curved vortex line segments and vortex sheet

elements are used. Through the movement and decay of these elements, as they interact with each other, the distorted rotor wake geometry is obtained.

Conservation of circulation dictates that the vorticity strength shed at specific spanwise locations behind each rotor blade is determined by circulation gradients on the blade. Spanwise circulation variations on rotor blade generate trailing vorticity, g_n, whose direction is parallel to the local flow velocity (figure 1). On the other hand, azimuthal variations produce shed vorticity radically oriented, g_s, due to the transient periodical nature of the rotor blade flowfield. Depending on its strength and its spanwise origin, the wake vorticity can form either concentrated vortex filaments or spread vortex layers.

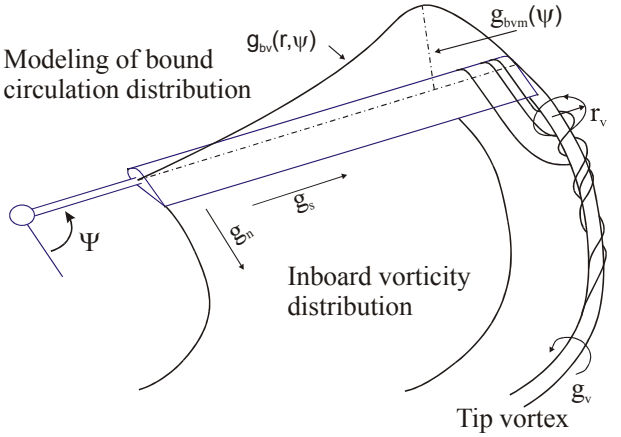

Fig. 1. Modeling of rotor blade bound circulation distribution and wake vorticity formations.

The strength of every vortex element used is derived from bound circulation distribution (figure 1). In general, the bound circulation curve can be assumed with a peak, g_{bvm}, near the blade tip while being zero at the tip itself. This steep gradient creates a high strength trailing vortex sheet, which rapidly rolls up and forms the concentrated tip vortex. Due to its strength, tip vortex dominates rotor wake flowfield and the accurate calculation of its geometry is the fundamental concern of any rotor wake flow simulation.

Inboard vorticity shed at blade's wake forms thin layers spread as long as the blade span. This part of rotor wake is created due to radial and azimuthal bound circulation variations for the trailing and shed wake vorticity respectively. With VEM implementation these parts of rotor wake are represented with vortex sheet elements [7].

The influence of wake vortices to rotor downwash can be computed utilizing potential theory relations, such as the Biot-Savart low. With known rotor downwash distribution, blade section aerodynamics can be calculated via a lifting line-blade element method, which is valid for the high aspect ratio helicopter rotor blades.

The present analysis assumes that the helicopter rotor performs a steady state equilibrium flight, implying that forward flight speed, rotor rotational speed, tip path plane orientation and wake geometry remain constant with time.

2.2 Rotor Aerodynamic Calculations

Distorted wake complexity makes the calculation of rotor downwash almost impossible with a direct numerical integration of the Biot-Savart law over the actual wake, and this procedure is used only for simplified approaches such as the rigid or semi-rigid wake assumptions.

The utilization of discrete computational elements (vortex lines and sheets) by VEM for rotor wake simulation, converts direct integration in a closed form integration of the Biot-Savart law over the known spatial locations of these elements. The contribution of a vortex line segment i to the induced velocity $\vec{w}_{ij}$ at an arbitrary point in space j, is given by the relation

$$\vec{w}_{ij} = -\frac{1}{4\pi}\int \frac{g_i\left(\vec{r}_{ijm} - k\cdot\vec{e}_k\right)\times d\vec{k}}{\left|\vec{r}_{ijm} - k\cdot\vec{e}_k\right|^3} \qquad (1)$$

where $\vec{r}_{ijm}$ is the minimum distance from vortex line i to the point j, $\vec{e}_k$ the unit vector in the direction of the vortex segment, g_i the circulation strength of the vortex segment and k the coordinate measured along the vortex segment. With a reasonable step of discretisation, the simplification made to the

actual wake geometry can be overcome.

Free wake computation is an iterative procedure, which initiates from rigid wake geometry. Each iteration defines a new position of each vortex element, taking in account the contributions of all the wake elements to local flow velocity. At the end of each iteration a new distorted wake geometry is calculated which is the starting point for the next circle. This scheme continues until distortion convergence is achieved. A picture of the final distorted wake geometry for a specific experimental test case is given in figure 2.

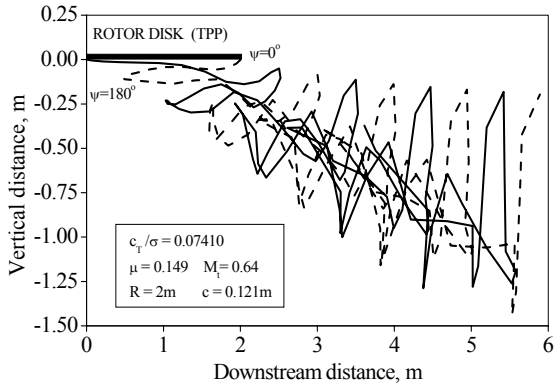

Fig. 2. Distorted free wake geometry calculation for an experimental test case of climb conditions. Two tip-vortices are shown for clarity starting from blade tips located at 0^o and 180^o of azimuth angle

Rotor blade dynamics influence the angle of attack distribution seen by the blade, and therefore alter the bound circulation distribution. Due to out-of-plane motion, rotor blade balances the asymmetry of rotor disk loading. For studying rotor aerodynamics and acoustics at low advance ratios, blade flapwise bending can be represented with a simple mode shape, without significant loss of accuracy.

In general the out of plane deflection z(r,t) can be written as a series of normal modes describing the spanwise deformation

$$z(r,t) = \sum_{k=1}^{\infty} n_k(r) q_k(t) \qquad (2)$$

where n_k is the mode shape and $q_k(t)$ is the corresponding degree of freedom. For the developed procedure only the first flapwise bending mode shape is used, $n=4r^2-3r$, which is appropriate for blade's basic bending deformation [16].

By these means a detailed rotor induced downwash distribution is obtained by free wake calculations. Sequentially, blade section angle of attack distribution is computed by

$$\alpha(r,\psi) = \theta(r) - tan^{-1}(u_P/u_T) \qquad (3)$$

where u_P is the air velocity perpendicular to No Feathering Plane (NFP) which includes nonuniform rotor downwash, u_T is the tangential velocity to blade airfoil, both normalized by tip speed ΩR, and $\theta(r)$ is the collective pitch angle (since NFP is taken as reference). With known angle of attack and local velocity, a blade-element type methodology is applied for blade section lift calculations. The above computational procedure is extensively documented in reference [7].

2.3 Vortex core modeling

Any computational procedure for rotor wake analysis includes a numerical representation of tip vortex structure and evolvement in the wake environment. A great deal of the current knowledge about these important aerodynamic issues has been derived mainly from experimental measurements. As a result empirical relations are commonly used for the determination of critical parameters for tip vortex physical modeling such as the vortex core radius, the velocity distribution at the core region and the viscous core growth.

Since VEM is based on a potential field solution such as Biot-Savart law for the calculation of the velocity induced by vortex elements to arbitrary points in space, singularities are expected to occur close to these elements. Due to the absence of viscosity effects, the velocity calculated in close proximity to these elements tends to be infinite. In order to remove these singularities and model the effects of viscosity in a convenient way the vortex core concept is introduced.

The core radius is defined as the distance from the core centre where the maximum tangential velocity is observed. A corresponding expression for the radial circulation distribution

inside the core region is introduced in the computations, which alters the velocity induced from a vortex element. Outside the core region the induced velocity has an approximately potential distribution which tends to coincide with the Biot-Savart distribution fairly away from the vortex line.

Several experimental and theoretical works have been presented [17,18,19] where velocity measurements have been taken in the core region and corresponding radial circulation distributions have been extracted. According to Vatistas [19] a series of tangential velocity profiles in the vortex core is given by the relation

$$V_\theta(r) = \frac{g\, r}{2\pi\left(r_c^{2n} + r^{2n}\right)^{1/n}} \qquad (4)$$

where g is the circulation of the vortex line, n is an integer variable, r is the radial distance from the vortex centre and r_c is the core radius. Using this relation for different values of n, the velocity profiles of some well-known core models can be derived using the nondimensional radius $\bar{r} = r/r_c$. For $n=1$ the core model of reference [20] is derived

$$V_\theta(\bar{r}) = \frac{g}{2\pi r_c}\frac{\bar{r}}{(1+\bar{r}^2)} \qquad (5)$$

For $n=2$ the model proposed in reference [21] by Bagai-Leishman is derived

$$V_\theta(\bar{r}) = \frac{g}{2\pi r_c}\frac{\bar{r}}{\sqrt{1+\bar{r}^4}} \qquad (6)$$

while vortex core radius was experimentally found to be between 5-7% of blade chord. A comparison of the above two vortex core models as well as Rankine and Lamp-Oseen [22] models, which were fitted in a least-square sense with experimental data, is given in [21]. The Kaufmann-Scully core model [20], is slightly underestimating the peak tangential velocity at early wake ages and improving later while the Bagai-Leishman vortex was in best agreement with experiments between the four models. With the application of vortex core circulation distribution, the velocity induced by the vortex elements is altered. Using the Kaufmann-Scully model the velocity induced to a point j from a finite straight vortex line segment i, of constant circulation g_i, with arbitrary orientation considering the relative geometrical distances $\vec{r}_{i1,j}$, $\vec{r}_{i2,j}$, is given as

$$\vec{w}_{i\,j} = \frac{g_i}{4\pi}\,\vec{r}_{i1,\,j} \times \vec{r}_{i2,\,j}\,\frac{N}{D} \qquad (7)$$

where

$$N = \left(\left|\vec{r}_{i1,j}\right| + \left|\vec{r}_{i2,j}\right|\right)\left[1 - \left(\vec{r}_{i1,j}\;\vec{r}_{i2,j}\right)/\left(\left|\vec{r}_{i1,j}\right|\left|\vec{r}_{i2,j}\right|\right)\right]$$

$$D = \left|\vec{r}_{i1,j}\right|^2\left|\vec{r}_{i2,j}\right|^2 - \left(\vec{r}_{i1,j}\;\vec{r}_{i2,j}\right)^2 +$$

$$+ r_c^2\left(\left|\vec{r}_{i1,j}\right|^2 + \left|\vec{r}_{i2,j}\right|^2 - 2\,\vec{r}_{i1,j}\;\vec{r}_{i2,j}\right)$$

For the present computational procedure both of the above core models Kaufmann-Scully and Bagai-Leishman were included as comparable options to describe the core of line and sheet vortex elements.

3 Numerical Blade Vortex Interaction Simulation

Blade Vortex Interactions are known crucial phenomena for helicopter rotor flowfield predictions. This is because they affect both the vortex filaments of rotor wake and the aerodynamics of rotating blades.

When a concentrated vortex comes very close to a rotating blade, experiences a sharp increase of its diameter so dramatic that is often mentioned as vortex core "bursting". The vorticity structure in the core region is influenced and the result is the enlargement of the core radius while the circulation of the vortex line is conserved. Several models have been developed to simulate this phenomenon and explain the associated effects on blade surface pressure distribution [1,4]. For the developed procedure the core "bursting" model is applied which imposes a steep increase of the vortex core radius. After numerical investigation and comparisons with experimental data, a burst core radius about 10 times the value of r_c was found to be adequate.

The bound circulation distribution is also

altered when a concentrated vortex passes in close proximity to a rotor blade due to sharp induced downwash fluctuations. The change of circulation produces an additional shedding of vorticity in the near wake behind this blade, which in terms affects the induced velocity distribution on the blade in an opposite manner than this of the concentrated vortex.

There are two main difficulties on applying a numerical model to predict the effects of this phenomenon on the computed blade downwash and circulation. First a minimum distance has to be defined so that every vortex filament closer than it to a rotor blade must be considered involved in a BVI event. This distance is denoted by h in figure 3 and its magnitude has to be externally imposed to the computations as a result of experimental observations and parametric numerical investigations. For the present work a value of 20 vortex core radii was found to give realistic predictions for blade aerodynamic magnitudes.

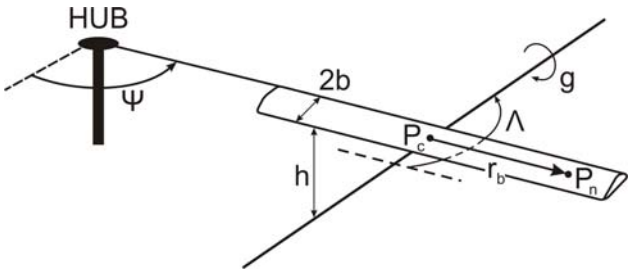

Fig. 3. Blade and vortex line relative positions for lifting surface theory solution.

The second difficulty comes from the fact that lifting line method cannot adequate describe the shedding of extra near wake due to local bound circulation changes. To account for these effects a formula, based on a lifting surface method proposed by Johnson [15], has been adopted.

The vortex-induced-airloads are calculated for an infinite aspect-ratio wing in a subsonic, compressible, freestream. A straight, infinite vortex interacts with the wing at an arbitrary angle Λ from the wing center line as shown in figure 3.

The circulation at any spanwise station P_n along the blade as a function of Mach number M, angle Λ, vertical distance h and spanwise distance r_b between BVI location P_c and station P_n is given by the relation

$$\frac{\Gamma(r_b \sin\Lambda)}{\frac{2\pi}{\alpha}Vb} = \frac{\Gamma_\infty}{2\pi Vb}\left\{-\sum_{n=0}^{2} a_n\left(\frac{d}{dr_b \sin\Lambda}\right)^{2n}\left[\frac{-(r_b \sin\Lambda+\cos\Lambda)}{(r_b \sin\Lambda+\cos\Lambda)^2+(h+c_n)^2}\right]+\right.$$

$$\sum_{n=0}^{1} a'_n\left(\frac{d}{dr_b \sin\Lambda}\right)^{2n}(-b_o)\left[-(r_b \sin\Lambda+\cos\Lambda)^2+(h+c'_n)^2+b_o^2\right]/ \qquad (8)$$

$$\left.\left[\left[-(r_b \sin\Lambda+\cos\Lambda)^2+(h+c'_n)^2+b_o^2\right]^2+4(r_b \sin\Lambda+\cos\Lambda)^2(h+c'_n)^2\right]\right\}$$

The expressions for determining the constants in equation (8) depend on the values of Mach number and angle Λ [23].

As already mentioned in previous paragraphs, VEM provides a transparent insight of rotor wake and blade flowfield. Taking advantage of this feature, the orientation of every vortex element relative to the interacting blade is computed and the BVI event can be designated as parallel, oblique or perpendicular. These designated numerical results of BVI type and location are compared to theoretical conclusions for different number of rotor blades and advance ratios.

A reliable prediction of the strength of each BVI event is another issue of numerical simulation. If a realistic picture of the location and strength of BVI events on rotor disk is numerically created, the factors that generate these phenomena can be traced and thoroughly examined. Well known factors that affect the multitude and intensity of BVIs are design parameters such as blade shape and rotor control inputs such as commanded pitch imposed to rotor blades. The former affects the circulation of the

trailing tip vortex and the later determines the orientation of rotor disk relative to the flight path. Especially for descending flight conditions where the number of BVIs increases, producing extensive noise emission and structural vibrations, numerical simulations can help to determine the optimum orientation of rotor disk for a given flight path.

4 Results and Discussion

One of the first simplified assumptions for rotor tip vortices geometry is the undistorted or 'rigid' wake geometry. This geometry is close to reality for the area just below rotor disk where each tip vortex is not seriously distorted by the velocity induced from its neighboring vortices. For this geometry the locations on rotor disk where BVI is possible to occur can be calculated by the relations

$$r\cos\left(\psi - \frac{2\pi(i-1)}{N_b}\right) = \cos(\psi - \delta) + \mu\delta \qquad (9)$$

$$r\sin\left(\psi - \frac{2\pi(i-1)}{N_b}\right) = \sin(\psi - \delta) \qquad (10)$$

where r is rotor radius, δ is the age of a point on tip vortex, ψ is the azimuth angle of the blade which created the vortex, N_b is the number of blades, μ is the advance ratio and $i = 0, .., N_b$.

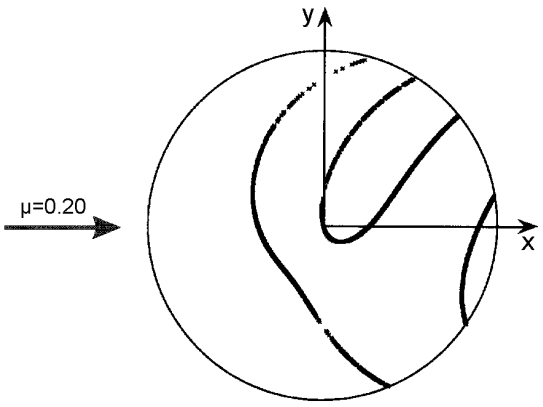

Fig. 4. Theoretical locus of all possible BVIs on rotor disk assuming rigid wake geometry in forward flight conditions (from reference [9]).

The values of (r, ψ) for which equations (9), (10) are simultaneously satisfied give the locus of all potential BVIs on rotor disk. For a two bladed rotor these locations are shown in figure 4.

These locations are calculated by the developed computational procedure for rigid wake geometry and are presented in figure 5 demonstrating the efficiency of the computations.

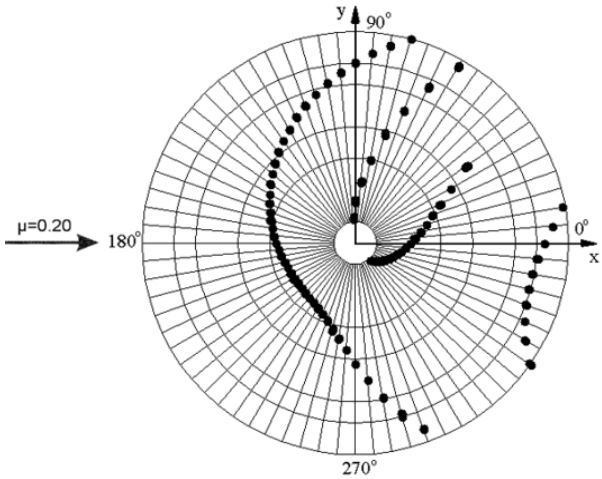

Fig. 5. Calculated locus of all possible BVIs on rotor disk assuming rigid wake geometry in forward flight conditions.

The actual geometry of a helicopter rotor wake is distorted compared to its initial helical form, because of flight velocity and the mutual interactions between tip vortices. The steady state distorted wake geometry is computed by an iterative procedure in which the starting scheme is rigid wake geometry.

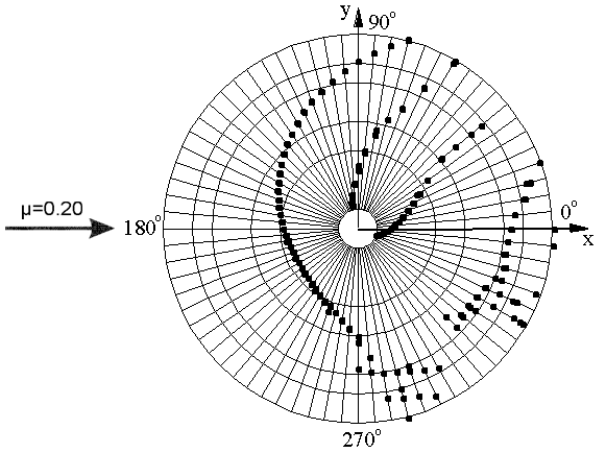

Fig. 6. Calculated locus of all possible BVIs on rotor disk based on distorted wake geometry in forward flight conditions.

The distortion of wake vortices changes the locus of the possible points where they intersect with rotor blades. To compare with the rigid wake case, figure 6 presents the computed possible BVI locations for the distorted geometry of the two-bladed rotor.

As can be seen in figure 6 the differences compared with the rigid wake case occur at the lateral sides of rotor disk, which is expected because the lateral distortion of tip vortices is greater as they pass closer to each other at these portions of rotor disk.

Helicopter flight conditions have a major effect on the number, location and intensity of BVI phenomena. In general tip vortices tend to evolve below rotor disk at the moment they emanate from blade tips. When the helicopter performs a descent flight, rotor is oriented nose-up while moving forward and tip vortices are forced to pass through the rotor disk. As a result the number of BVIs is substantially increased and descent flights are known to produce intense noise and vibrations.

In an opposite manner, experimental observations show that climb flight conditions produce low noise levels and reduced blade vibrations. Flow visualization results for such cases [11] lead to the conclusion that due to flight conditions, tip vortices depart from the area below the rotor just after their formation and they don't interact as much with the rotating blades.

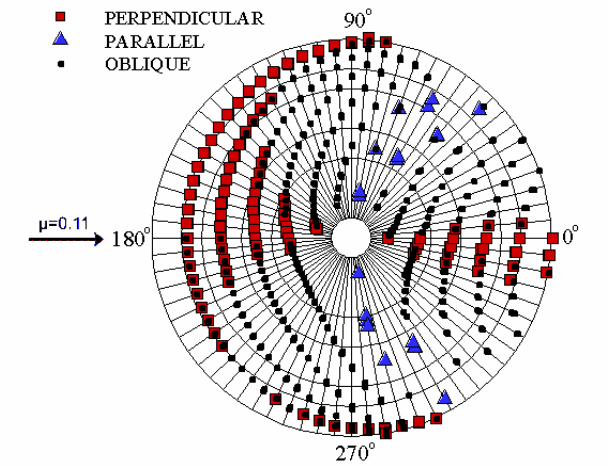

Fig. 7. Locus of calculated BVI events for a distorted wake geometry and descent flight conditions with c_T/σ =0.0571, μ=0.11, α_{TPP}=11.87° and M_t=0.64.

Simulated flight conditions for several experimental test cases show that computational results obtained by the developed procedure, are in accordance with the above observations for BVIs number and locations. The following figures present computed BVI locus for one level case and two descent cases with varying descending angle (positive tip path plane angles correspond to nose up orientation of rotor disk).

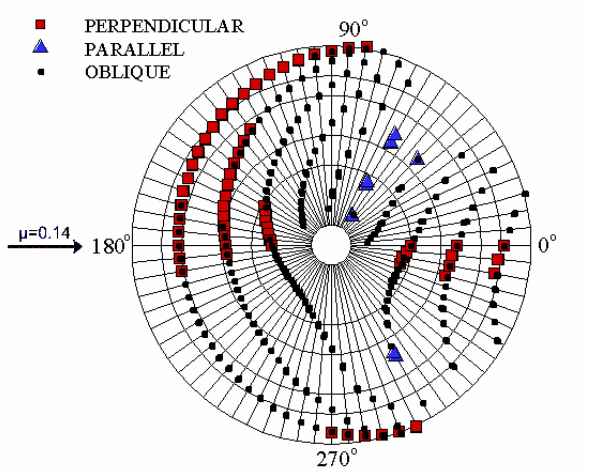

Fig. 8. Locus of calculated BVI events for a distorted wake geometry and descent flight conditions with c_T/σ =0.0571, μ=0.14, α_{TPP}=6.8° and M_t=0.64.

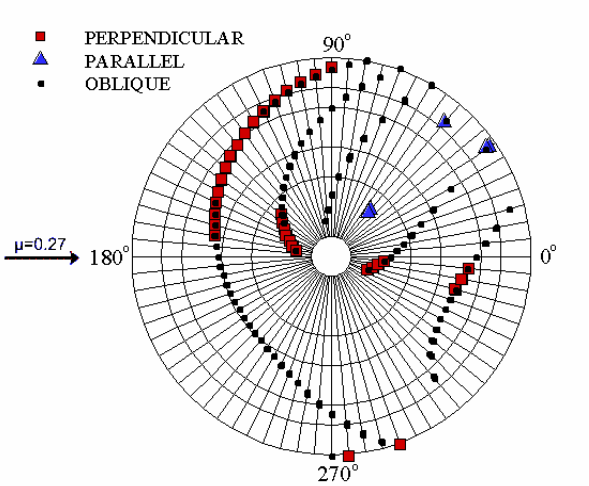

Fig. 9. Locus of calculated BVI events for a distorted wake geometry and level flight conditions with c_T/σ =0.0571, μ=0.27, α_{TPP}=-1.0° and M_t=0.64.

As shown in the above figures, computations verify what is already discussed. Level flight has the smallest number of BVIs and they are mostly gathered at the advancing

side of rotor disk. This means that at small ages after their shedding, tip vortices interact with the following blades mostly in perpendicular orientation.

Figures 7 and 8 demonstrate the influence of increasing descent angle on BVI number and locations. A notice can be made about the prediction of BVIs in parallel orientation relative to rotor blade for the highly descending conditions with 11.87° descent angle [11].

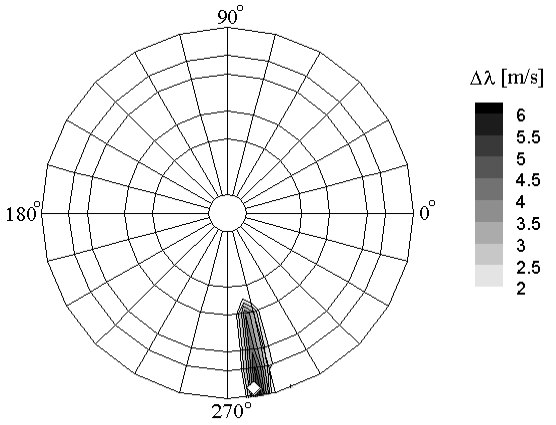

Fig. 10. Contours of downwash velocity changes when including and excluding an isolated BVI event. The intensity of the specific event and its influence on downwash distribution is demonstrated.

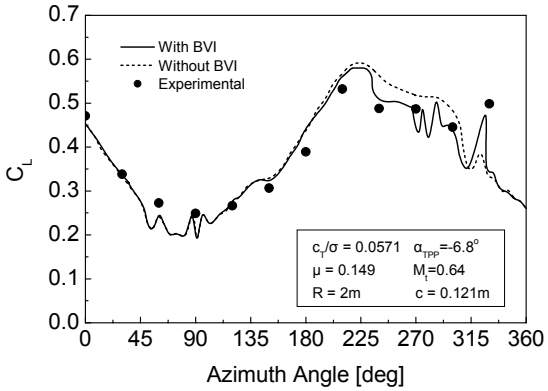

Fig. 11. Comparison of azimuthal blade section lift distribution for including and excluding an isolated BVI event for an experimental test case of climb flight conditions.

These specific interactions are predicted mostly at the advancing side which is consistent with observations mentioned in reference [9].

The influence of an isolated BVI event is shown in the contour plot of figure 10. The downwash distributions at the area of the calculated BVI location for the cases of including and excluding this particular BVI event are computed and their differences are contoured in figure 10.

For the BVI event shown in previous figure, the corresponding changes in blade section lift coefficient are shown in figure 11.

Load fluctuations because of blade surface pressure changes are calculated when the BVI event is taken into account as expected and in this case the agreement with the experimental data for blade section lift is fairly improved.

By these means, numerical BVI simulation can help to locate areas on rotor disk which generate intense BVI noise and blade fatigue for predetermined flight conditions.

References

[1] Horner M B, Galbraith R A, Coton F N, Stewart J N, and Grant I. Examination of vortex deformation during blade-vortex interaction. *AIAA Journal*, Vol. 34, No. 6, pp 1188-1194, 1996.

[2] Wittmer K S, and Devenport W J. Effects of perpendicular blade-vortex interaction part1: turbulence structure and development. *AIAA Journal*, Vol. 37, No. 7, pp 805-817, 1999.

[3] Kitaplioglu C, and Caradonna F. Aerodynamics and acoustics of blade-vortex interaction using an independently generated vortex. *American Helicopter Society Aeromechanics Specialists Conference*, San Francisco CA, 1994.

[4] Rahier G, and Delrieux Y. Influence of vortex models on blade-vortex interaction load and noise predictions. *Journal of American Helicopter Society*, Vol. 44, No. 1, pp 26-33, 1999.

[5] Rule J A, Epstein R J, and Bliss D B. Unsteady compressible boundary element calculations of parallel blade-vortex interaction. *Journal of American Helicopter Society*, Vol. 44, No. 4, pp 302-311, 1999.

[6] Caradonna F, Kitaplioglou C, McCluer M, Baeder J, Leishman G J, Berezin C, Visintainer J, Bridgeman J, Burley C, Epstein R, Lyrintzis A, Koutsavdis E, Rahier G, Delrieux Y, Rule J, and Bliss D. Methods for the prediction of blade-vortex interaction noise. *Journal of American Helicopter Society*, Vol. 45, No. 4, pp 303-317, 2000.

[7] Spyropoulos A I, Fragias A P, Papanikas D G, and Margaris D P. Influence of arbitrary vortical wake evolution on flowfield and noise generation of helicopter rotors. *22nd Congress of International*

Council of the Aeronautical Sciences, Harrogate U K, Paper ICAS 0394, pp 394.1-394.15, 2000.

[8] Krishnamoorthy S, and Marshall J S. Three-dimensional blade-vortex interaction in the strong vortex regime. *Physics of Fluids*, Vol. 10, No. 11, pp 2828-2845, 1998.

[9] Leishman G. *Principles of Helicopter Aerodynamics*, 1st edition, Cambridge University Press, 2001.

[10] Johnson W. Calculation of blade-vortex interaction airloads on helicopter rotors. *Journal of Aircraft*, Vol. 26, No. 5, pp. 470-475, 1988.

[11] Splettstoesser W R, Niesl G, Cenedese F, Nitti F, and Papanikas D G. Experimental results of the european HELINOISE aeroacoustic rotor test. *Journal of American Helicopter Society*, Vol. 40, No. 2, 1995.

[12] Ahmad J, and Duque E. Helicopter rotor blade computation in unsteady flows using moving overset grids. *Journal of Aircraft*, Vol. 33, No. 1, pp 54-60, 1996.

[13] Chorin A J. *Computational Fluid Mechanics*, 1st edition, Academic Press, 1989.

[14] Bliss D B, Teske M E, Quackenbush T R. *A New Methodology for Free Wake Analysis Using Curved Vortex Elements*, NASA CR-3958, 1987.

[15] Johnson W. *A Comprehensive Analytical Model of Rotorcraft Aerodynamics and Dynamics*, NASA TM-81182, 1980.

[16] Johnson W. *Helicopter theory*, 1st edition, Princeton University Press, 1980, 2nd edition, Dover, 1994.

[17] Bhagwat J M, and Leishman G J. Correlation of helicopter rotor tip vortex measurements. *AIAA Journal*, Vol. 38, No. 2, pp. 301-308, 2000.

[18] Windnall S E, and Wolf T L. Effect of tip vortex structure on helicopter noise due to blade vortex interactions. *AIAA Journal of Aircraft*, Vol. 17, No. 10, pp. 705-711, 1980.

[19] Vatistas G H, Kozel V, and Mih W C. A simpler model for concentrated vortices. *Experiments in Fluids*, Vol. 11, pp.73-76, 1991.

[20] Scully M P. *Computation of helicopter rotor wake geometry and its influence on rotor harmonic airloads*, ASRL TR 178-1, 1975.

[21] Leishman G J, Baker A, and Coyne A. Measurements of rotor tip vortices using three-component laser doppler velocimetry. *Journal of American Helicopter Society*, Vol. 41, No. 4, pp. 342-353, 1996.

[22] Lamb H. *Hydrodynamics*. 6th Edition, Cambridge University Press, 1932.

[23] Johnson W. A lifting surface solution for vortex induced airloads. *Journal of Aircraft*, Vol. 9, No. 4, pp. 689-695, 1971.